International Journal of Environment and Geoinformatics (IJEGEO) is an international, multidisciplinary, peer reviewed, open access journal.

A Spectral Band Based Comparison of Unsupervised Segmentation Evaluation Methods for Image Segmentation Parameter Optimization

Hasan TOMBUL, Taşkın KAVZOĞLU

Reaserch Article

A Spectral Band Based Comparison of Unsupervised Segmentation Evaluation Methods for Image Segmentation Parameter Optimization

Hasan Tonbul [*] iD **, Taşkın Kavzoğlu** iD

Gebze Technical University, Department of Geomatics Engineering, 41400, Kocaeli, TR

* Corresponding author:H. Tonbul
E-mail: htonbul@gtu.edu.tr

Abstract

Very high-resolution images obtained with recently launched satellite sensors have been used intensively in the remote sensing area. The widespread use of high-resolution images has greatly facilitated the creation and updating of land use/land cover (LULC) maps. Traditional pixel-based image analysis methods that extract information based solely on the spectral values of pixels are generally not suitable for high-resolution images. Unlike pixel-based approaches, object-based image analysis (OBIA) uses pixel clustering (image objects) instead of pixels by considering the shape, texture, context and spectral features and provides richer information extraction. Image segmentation is an important process and prerequisite for the OBIA process. It is essential to evaluate the performance of segmentation algorithms for the determination of effective segmentation methods and optimization of segmentation parameters. In this study, the multi-resolution segmentation algorithm is used for the segmentation process. The effect of spectral bands on segmentation quality was analysed using a Worldview-2 high-resolution satellite image. In order to analyse segmentation quality, two unsupervised quality metrics, namely, F-measure and Plateau Objective Function (POF) values were calculated for each band separately. In this manner, optimum parameter values were determined using different variations of Moran's I Index and variance values. Image segmentation was performed by using different scale, shape and compactness parameter values. In this context, 30 segmentation analyses were performed considering three different spectral bands (red, green and near-infrared bands). The results showed that the highest segmentation quality was acquired for the NIR band among the spectral bands for the F-measure method, while the highest segmentation quality value was achieved for the green band for the POF metric. In addition, the optimum segmentation parameter values of the scale, shape and compactness were determined as 30-0.3-0.5 and 50-0.1-0.3, for F-measure and POF approaches, respectively.

Introduction

Thematic map generation through land use/land cover (LULC) classification is one of the most important and widely used applications in the analysis of remote sensed data (Kavzoğlu and Cölkesen, 2013). Especially, with the possibilities offered by high spatial resolution remote sensing systems such as Worldview, IKONOS and QuickBird, the object-based image analysis (OBIA) approach has come to the forefront (Blaschke et al., 2004; 2008; Hossain and Chen, 2019). In this approach, instead of handling pixels individually, similar and adjacent clusters of pixels are addressed, and the analysis is performed on image clusters (objects). In this way, the data size is reduced compared to the use of pixels individually, and more importantly, not only spectral properties of the pixels but also shape, texture, context and spectral features of extracted image objects considered for image analysis (Kavzoğlu, 2017; Algancı et al., 2018; Esetlili, et al., 2018). OBIA mainly consists of two steps: dividing the image into segments or different image objects and classifying the generated image segments.

Segmentation creates spatial and spectrally homogeneously defined image objects and enables visual image interpretation (Blaschke, 2010; Jensen 2016). The determination of effective segmentation methods has enormous importance for OBIA. However, selection of an efficient segmentation method and its parameters is a very difficult task depending on the texture, size and complex structure of the earth objects (Johnson and Xie, 2011). When an appropriate and efficient segmentation approach is not preferred, over-segmentation and under-segmentation may arise (Su, 2019). Therefore, optimum methods for image segmentation quality assessment are required. The evaluation of segmentation quality and determination of appropriate segmentation parameters are performed into three main categories: visually, supervised and unsupervised approaches (Zhang, 1996; Zhang et al., 2008). The visual methods are mainly based on the user performing particular segmentations and a visual assessment of the produced segmentation quality results. (Grybas et al., 2017). However, this method is generally considered highly subjective and time consuming (Johnson and Xie, 2011). On the other hand, supervised and unsupervised methods are considered less subjective than visual evaluations, and once automated,

many segments can be evaluated at a time and can be cost effective for image analysis (Grybas et al., 2017). In addition, it has been stated in many studies that high accuracy can be achieved according to selection of optimal segmentation parameter and segmentation method (Clinton et al. 2010; Gao et al. 2011; Kavzoğlu et al., 2017; Kavzoğlu and Tonbul, 2018). Supervised methods evaluate segmentation quality by quantitively evaluating the relationship between user-generated reference polygons and generated image objects. Unsupervised evaluation methods do not use reference polygons, but several image statistics are used to evaluate segmentation quality. In addition, intra-segment and inter-segment evaluation methods (e.g., variance and spatial autocorrelation) are used in unsupervised approaches to determine segmentation quality (Martha et al., 2011; Yang et al., 2015).

In this study, two unsupervised evaluation methods, namely, F-measure and Plateau Objective Function (POF) methods were performed using different segmentation parameters on a heterogeneous Worldview-2 image. Considering the image characteristics, it is considered that the unsupervised approach would be more appropriate for this study since no reference data set was needed and the use of intra-segment and inter-segment heterogeneity information would be more appropriate. This study has two main objectives: i) to investigate the effect of three spectral bands (red, green, and near infrared) on image segmentation quality, ii) to determine the optimal combination of segmentation parameters.

Study Area and Dataset

In this study, Worldview-2 satellite image acquired on July 12, 2012, which includes a part of Gebze district of Kocaeli province, was used (Fig. 1). The image of the study area covers an area of 5500x8000 pixels and has similar spectral characteristics in terms of LULC classes. The Worldview-2 image has eight multispectral (red, green, blue, near-infrared-1, near infrared-2, yellow, red edge and coastal) and a panchromatic band, with a 2-meter multispectral and 0.5-meter panchromatic spatial resolution. In this study, pan-sharpened image was used. The Gram-Schmidt pan-sharpening algorithm was used in the fusion of panchromatic and multispectral bands and the nearest neighbor resampling technique was used in image analysis. The image segmentation process was performed using Definiens eCognition Developer software. Furthermore, MATLAB and ArcGIS software packages were used to calculate Moran's I and local variance values.

Methodology

Multi-resolution Segmentation

In this study, multi-resolution image segmentation algorithm, proposed by Baatz and Schäpe (2000), one of the most used and most effective segmentation algorithm in literature, was employed.
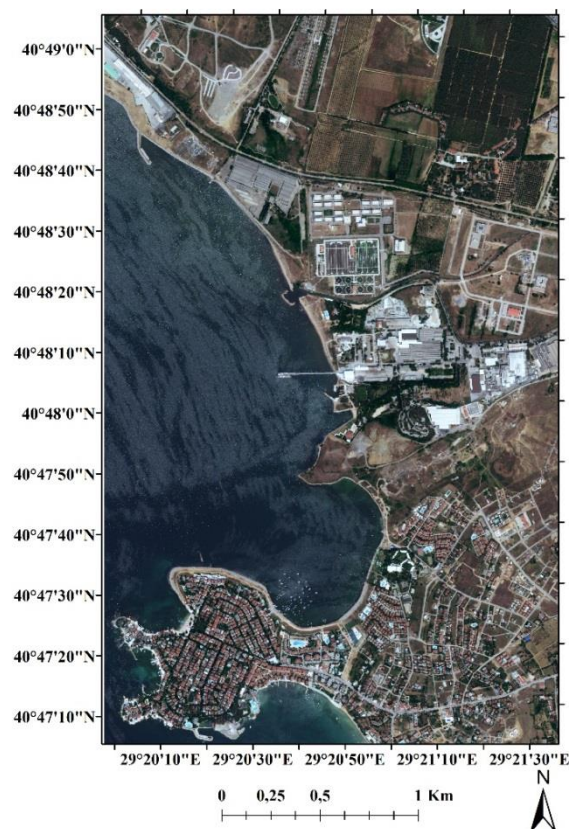

Fig. 1. The Worldview-2 imagery of the study area, Gebze District of Kocaeli, Turkey.

The multi-resolution algorithm is a region-based segmentation algorithm based on local homogeneity criteria. This process starts with a single pixel and collects pixels of different shapes, sizes and properties in the form of image objects until a user-defined homogeneity level or threshold is reached. Thus, the maximum heterogeneity for the generated image objects is determined (Baatz and Schäpe, 2000). Multi-resolution segmentation consists of three main parameters: scale, shape, and compactness. The scale parameter is considered to be the most effective factor that controls the average image object size. As the scale value increases, the image object size also increases. (Kavzoğlu and Tonbul, 2018). The shape parameter affects the decomposition of LULC classes based on color and texture information, and the compactness parameter helps to define the image object boundaries sharper and smoother. It should be also noted that the values of the shape and compactness parameters range between 0 and 1.

Evaluation of Segmentation Quality

In order to investigate the segmentation quality evaluation of different multi-resolution segmentation combinations, two unsupervised segmentation evaluation methods, namely, F-measure and POF method were utilized. Based on the level combinations of multi-resolution segmentation parameters (scale, shape, compactness), F-measure and POF values were calculated for each parameter combination. The F-measure determines the relative effects of normalized Moran's I and variance, and thus the level of over-

segmentation and under-segmentation by using an adjustable weight degree (Johnson et al., 2015). The F-measure equation is determined by calculating Moran's I and variance and the formula is expressed as follows:

$$MI = \frac{n\sum_{i=1}^{n}\sum_{j=1}^{n}w_{ij}(y_i-\overline{y})(y_j-\overline{y})}{\sum_{i=1}^{n}(y_i-\overline{y})^2(\sum\sum_{i\neq j}w_{ij})}$$

(Eq.1)

where n illustrates total number of regions, w_{ij} shows measure of the spatial adjacency of regions R_i and R_j, y_i is the mean spectral value of region R_i, and $\overline{y}$ is the mean spectral value of the image. It should be noted that if R_i and R_j are adjacent, $w_{ij}=1$, else $w_{ij} = 0$. Furthermore, Moran's I range from -1 (dispersed) to +1 (clustered). Low Moran's I values show high inter-segment heterogeneity, which is anticipated for an image segmentation.

$$V = \frac{\sum_{i=1}^{n}a_i \cdot v_i}{\sum_{i=1}^{n}a_i}$$

(Eq. 2)

where v_i illustrates variance of a segment and a_i shows the area of region i. Since Moran's I and variance take different values, normalization process should be performed to equally consider both metrics.

$$F(x) = \frac{x-x_{\min}}{x_{\max}-x_{\min}}$$

(Eq. 3)

where x_{min} and x_{max} refers to the minimum and maximum values of Moran's I or variance.

$$F\text{-}measure = (1+a^2)\frac{MI_{norm} x\ V_{norm}}{a^2\ x\ MI_{norm}+V_{norm}}$$

(Eq.4)

where a is a weight that regulate the relative weights of MI_{norm} and V_{norm}. For instance, $a = 1$ illustrates equal weighting for MI_{norm} and V_{norm}, while $a = 0.5$ shows semi weighting for V_{norm} (Johnson et al., 2015). F-measure values range from 0 to 1, and higher values indicate better segmentation quality. The second metric used in this study is POF, which is a combination of variance and Moran's I, proposed by Espindola et al. (2006) given by:

$$POF = MI_{norm}+V_{norm}$$

(Eq.5)

It should be noted that lower values of POF metric show better segmentation quality.

Table 1. The multi-resolution segmentation parameters and combinations

Combination	Scale	Shape	Compactness
1	10	0.1	0.3
2	10	0.1	0.5
3	10	0.1	0.7
4	10	0.1	0.9
5	10	0.3	0.1
6	10	0.3	0.5
7	10	0.5	0.1
8	10	0.5	0.3
9	10	0.7	0.1
10	10	0.7	0.3
11	30	0.1	0.3
12	30	0.1	0.5
13	30	0.1	0.7
14	30	0.1	0.9
15	30	0.3	0.1
16	30	0.3	0.5
17	30	0.5	0.1
18	30	0.5	0.3
19	30	0.7	0.1
20	30	0.7	0.3
21	50	0.1	0.3
22	50	0.1	0.5
23	50	0.1	0.7
24	50	0.1	0.9
25	50	0.3	0.1
26	50	0.3	0.5
27	50	0.5	0.1
28	50	0.5	0.3
29	50	0.7	0.1
30	50	0.7	0.3

Results

In this study, the effect of three spectral bands (red, green, and NIR) on segmentation quality was investigated on multi-resolution segmentation using high-resolution Worldview-2 image. In this manner, two unsupervised quality methods (i.e., POF and F-measure) were calculated for 30 multi-resolution segmentation parameter combinations to determine optimal multi-resolution segmentation parameters. Table 1 shows the parameter values and combinations used for multi-resolution image segmentation.
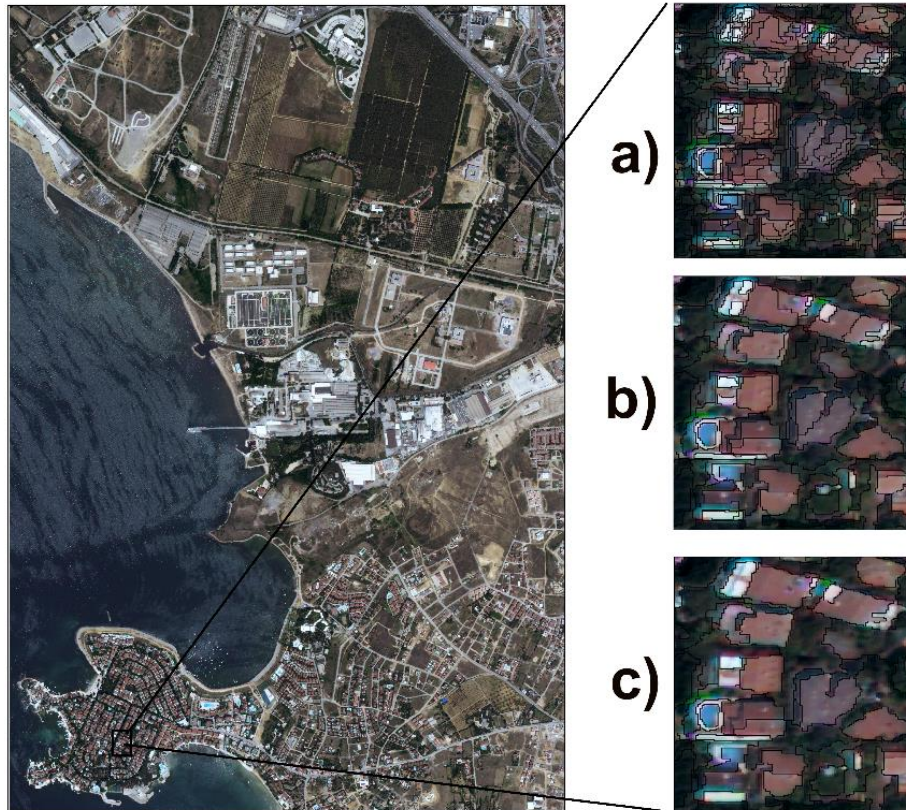

Fig. 2. A subset of visual comparison created by (a) combination 10, (b) combination 20, (c) combination 30.

It should be noted that the selection of the specified scale parameter values was determined by trial-and-error method to avoid over segmentation or under segmentation. In the selection of shape and compactness parameters, more frequently used combinations in the literature were preferred (Aguilar et al., 2016; Saba et al., 2016; Cökesen and Kavzoğlu, 2017; Tonbul and Kavzoğlu, 2019). Furthermore, image objects were created by taking all band weights equal while performing image segmentation. The image segmentation process using three sample segmentation parameter combinations is shown on subset image of Worlview-2 image (Fig. 2).

When the result of segmentation obtained in Fig. 2(a) was examined, it was observed that some image objects were exposed to over-segmentation while in Fig. 2 (c) it was seen that some image objects were exposed to under-segmentation. On the other hand, Fig. 2(b) shows that the created image objects correspond relatively better with real-earth objects compared to other segmentation results. After obtaining 30 different levels of image segments on the Worldview-2 image, the F-measure and POF values were calculated separately for the determination of the optimum scale parameter. For each produced segmentation image, Moran's I (MI) and Variance (V) values were calculated separately for the NIR, green and red spectral bands. In order to compare the calculated Moran's I and variance values in the same range, normalization process was applied, and the normalized values were rescaled between range 0 and 1. Fig. 3 represents the variation between normalized Moran's I and variance values.

As can be seen from Figure 3, similar results were obtained for all band combinations and normalized Moran's I values tend to decrease while variance values tend to increase. Segmentation results for all combinations of MRS parameters were estimated by calculating their POF and F-measure values, as shown in Table 2.
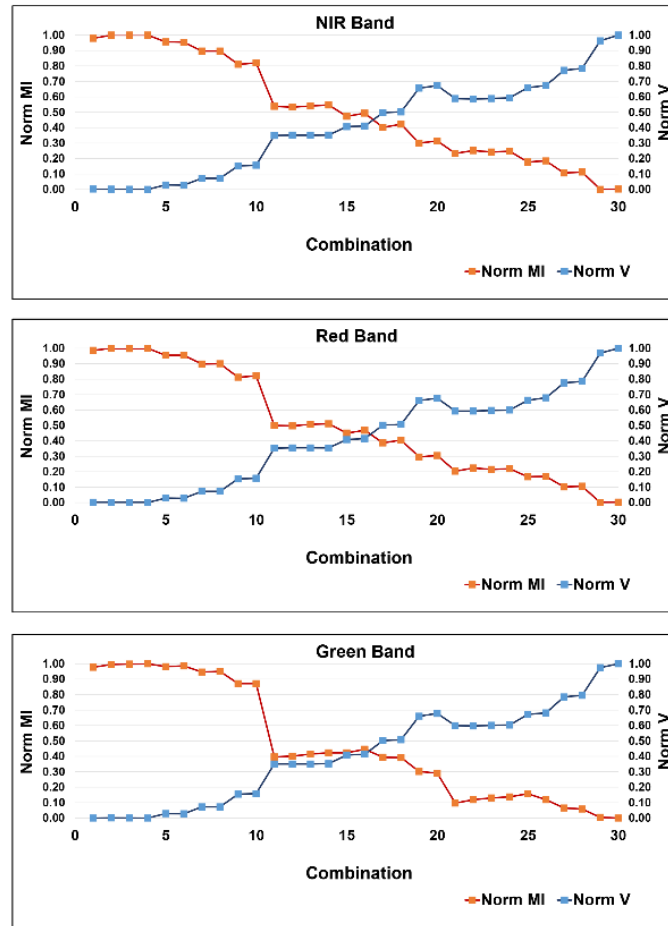
Fig. 3. Graphical representation of normalized variance and normalized Moran's I values for three spectral bands.

Table 2. Summary of multi-resolution segmentation parameter combinations from POF and F-measure values

	NIR Band		Red Band		Green Band		Three Band Average	
Combination	POF	F-measure	POF	F-measure	POF	F-measure	POF	F-measure
1	0.982	0.005	0.988	0.003	0.978	0.000	0.982	0.003
2	1.001	0.002	1.001	0.003	0.997	0.002	1.000	0.003
3	1.001	0.001	0.998	0.002	0.998	0.001	0.999	0.001
4	1.000	0.000	1.000	0.000	1.000	0.000	1.000	0.000
5	0.985	0.057	0.984	0.057	1.011	0.056	0.993	0.056
6	0.982	0.054	0.983	0.054	1.014	0.054	0.993	0.054
7	0.968	0.133	0.971	0.135	1.019	0.135	0.986	0.134
8	0.968	0.133	0.973	0.134	1.023	0.135	0.988	0.134
9	0.963	0.256	0.966	0.259	1.027	0.263	0.985	0.260
10	0.976	0.263	0.979	0.264	1.031	0.269	0.995	0.265
11	0.887	0.424	0.853	0.414	0.747	0.372	0.829	0.403
12	0.885	0.424	0.853	0.414	0.751	0.374	0.830	0.404
13	0.892	0.426	0.862	0.418	0.765	0.380	0.840	0.408
14	0.900	0.429	0.866	0.419	0.776	0.385	0.847	0.411
15	0.880	0.438	0.859	0.428	0.832	0.416	0.857	0.427
16	0.925	**0.459**	0.912	**0.450**	0.899	**0.442**	0.883	**0.450**
17	0.900	0.445	0.889	0.437	0.896	0.441	0.895	0.441
18	0.905	0.449	0.883	0.440	0.859	0.429	0.912	0.439
19	0.957	0.412	0.958	0.409	0.962	0.414	0.959	0.412
20	0.987	0.428	0.982	0.421	0.968	0.407	0.979	0.419
21	**0.822**	0.334	**0.797**	0.303	**0.696**	0.167	**0.772**	0.268
22	0.837	0.352	0.817	0.325	0.716	0.199	0.790	0.292
23	0.832	0.344	0.812	0.316	0.732	0.215	0.792	0.291
24	0.841	0.349	0.820	0.321	0.740	0.224	0.800	0.298
25	0.837	0.280	0.830	0.267	0.829	0.255	0.832	0.268
26	0.858	0.290	0.849	0.272	0.801	0.203	0.836	0.255
27	0.878	0.187	0.877	0.180	0.850	0.121	0.869	0.162
28	0.897	0.198	0.892	0.187	0.854	0.109	0.881	0.165
29	0.963	0.000	0.969	0.000	0.979	0.009	0.970	0.003
30	1.002	0.005	1.002	0.005	1.000	0.000	1.002	0.003

It should be noted that the bold values in Table 2 represent the optimum MRS parameter levels for POF and F-measure, showing the lowest POF and highest F-measure values. According to the results, the optimal F-measure values were obtained as 0.442 for green band, 0.450 for red band and 0.459 for NIR band. On the other hand, the optimal POF values were obtained as 0.696 for green band, 0.797 for red band and 0.822 for NIR band. When the results were examined, it was observed that the highest segmentation quality was obtained for the NIR band (0.459) among the spectral bands for the F-measure method, while the highest segmentation quality value was obtained for the green band (0.696) for the POF method. Furthermore, three band average of POF and F-measure values comparison with single band of POF and F-measure values were presented in Table 2. Another important finding was that optimal segmentation parameter values for all bands were obtained at combination-16 for F-measure method and combination-21 for POF method. In other words, the scale, shape and compactness parameter values were found to be 30-0.3-0.5 and 50-0.1-0.3, for F-measure and POF approaches, respectively.

According to optimum parameter combinations of POF (i.e, combination-21), and F-measure (i.e, combination-16), method (i.e combination-16), totally 150,654 image segments were created by combination-16 and 86,690 image segments were produced by combination-21 method. It was seen that there were approximately 64,000 segment differences between the two methods. As it is known, the increase in the number of segments increases the processing time and data size for the subsequent classification analysis. Therefore, it was observed that the use of POF method may be more suitable than the F-measure method compared to created number of segments for subsequent image analysis. Furthermore, three sample sites for optimal parameter combinations generated by F-measure and POF methods were extracted and shown as zoomed in Fig. 4 for visual comparison of two methods.

As shown in figure, it has been observed that the produced segments for both methods are very similar to each other and that the segment boundaries overlap well with the earth objects, but some segments exhibited dissimilarities for delineation of LULC classes objects compared to each method. The results of POF and F-measure values between spectral bands for all segmentation combinations are given in Fig. 5.
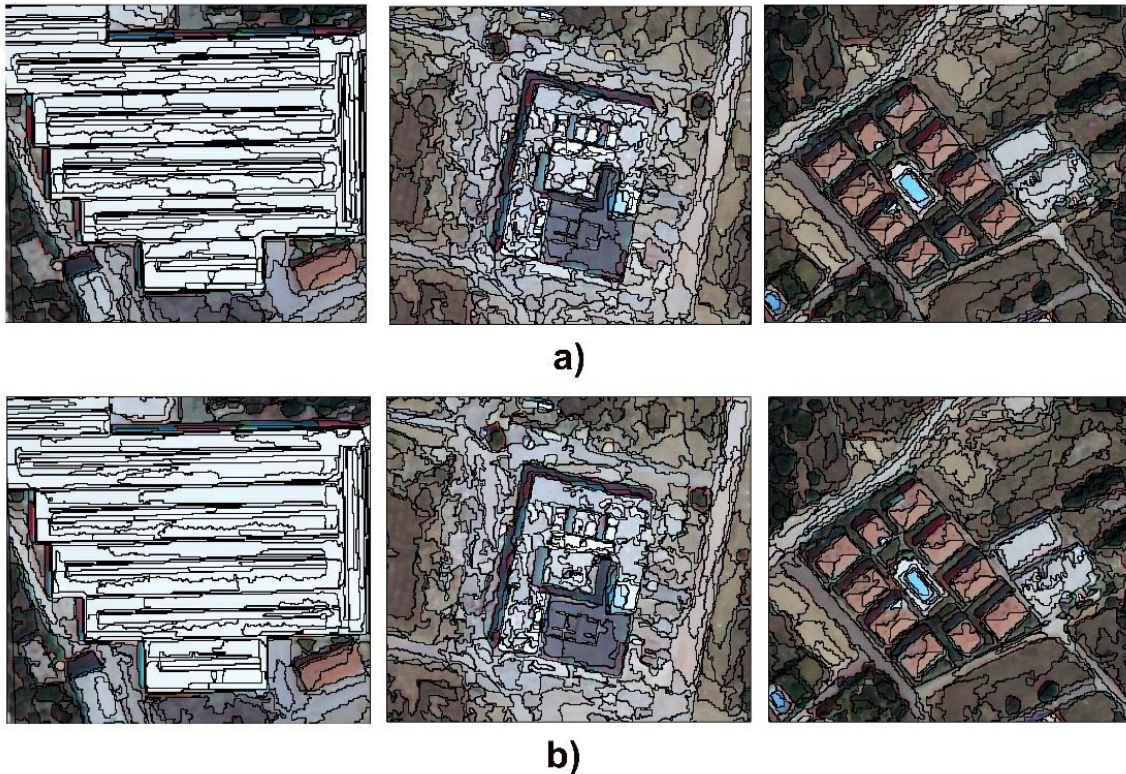

Fig. 4. Comparison of selected sample sites produced by optimal parameter combinations for: a) F-measure method (combination-16), b) POF method (combination 21)
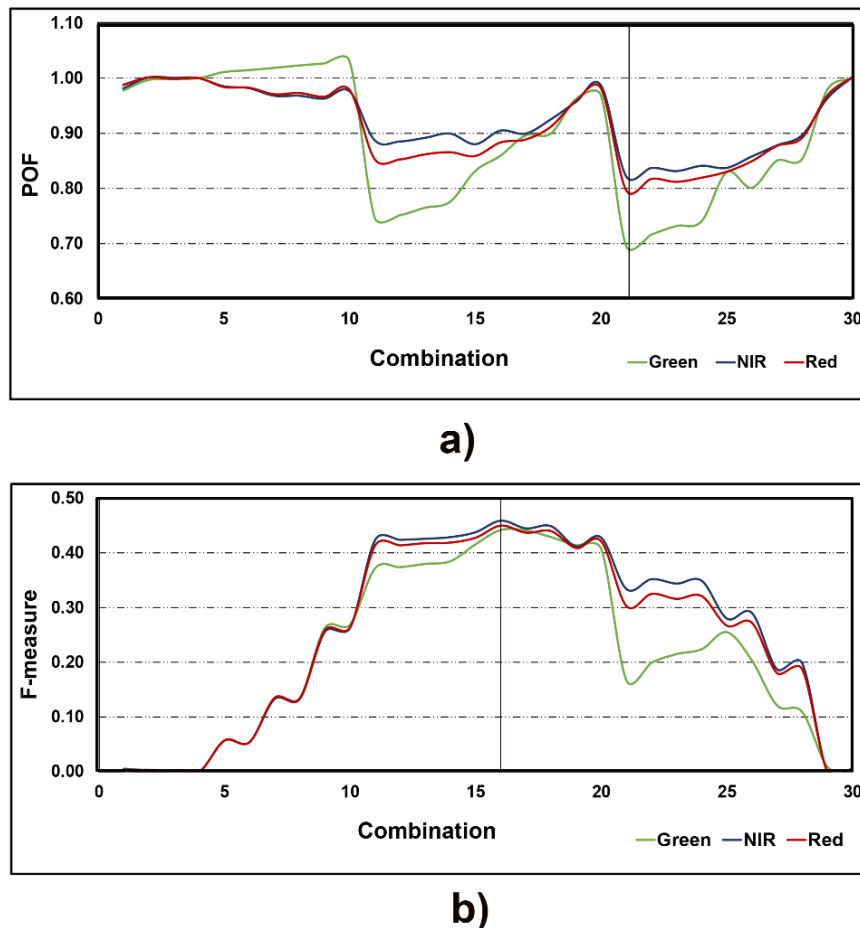
a)

b)

Fig. 5. The parameter combinations of spectral bands according to (a) POF and (b) F-measure values.

As can be seen from the Fig. 5(a), all spectral bands between combination 1-5 yielded very similar results, while it was seen that there are some divergences between bands between combination 5-15 and 20-30. Furthermore, as shown in Fig. 5(b), it was observed that all spectral bands between combinations 1-10 give very similar results, while it was seen that there are some divergences between bands between combination 10-15 and 20-25. In addition, the highest segmentation quality results for the F-measure method were calculated in the combination 15-20 range, while the highest segmentation quality results for the POF method were calculated in the combination 20-25 range.

Conclusion

In this study, the effects of segmentation quality on various segmentation parameters were investigated using two unsupervised segmentation evaluation methods, namely POF and F-measure. Within the scope of the study, a multi-resolution segmentation parameter combination of 30 different values were tested separately on three different spectral bands (i.e. red, green and NIR) of the Worldview-2 high resolution image. Thus, the optimum combination of parameters and the effects of spectral bands on segmentation quality were analyzed in detail by correlating them with variance and Moran's I values. The following conclusions can be drawn from the present study. First, it was determined that normalized variance and normalized Moran's values showed inversely proportional behavior on different segmentation parameters. Second, it was observed that the NIR band provided better segmentation quality accuracy compared to other bands for the F-score method, while the green band provided better segmentation quality accuracy than the other bands for POF method. Third, it was seen that the best segmentation results for all band combinations were observed in the combination range of 15-20 for the F-measure approach, while the best segmentation results for all band combinations were determined in the combination range of 20-25 for POF approach. According to the optimum setting for multi-resolution using POF and F-measure values were estimated as 50-0.1-0.3 and 30-0.5-0.3 for scale, shape and compactness parameters, respectively. Furthermore, when the visual interpretations and the number of segments produced are analyzed, it is seen that the POF method may be a better segmentation quality evaluation method than the F-measure method. Further investigations are required to validate the performance of segmentation evaluation metrics in different types of data sets.

References

Aguilar, M.A., Aguilar, F.J., García Lorca, A., Guirado, E., Betlej, M., Cichon, P., Nemmaoui, A., Vallario, A., Parente, C. (2016). Assessment of multiresolution seg-mentation for extracting greenhouses from WorldView-2 imagery. International Archives of the Photogrammetry, *Remote Sensing and Spatial Information Sciences* (ISPRS archives) 41, 145-152.

Algancı, U , Sertel, E , Kaya, Ş. (2018). Determination of the Olive Trees with Object Based Classification of Pleiades Satellite Image. *International Journal of Environment and Geoinformatics,* 5 (2) , 132-139. DOI: 10.30897/ijegeo.396713

Baatz, M., Schape, A. (2000). Multiresolution segmentation – An optimization approach for high quality multi-scale image segmentation. In: Strobl J. et al. (Eds.), Angewandte *Geographische Informationsverarbeitung* (pp. 12–23), Herbert Wichmann Verlag.

Blaschke, T. (2010). Object based image analysis for remote sensing. *ISPRS Journal of Photogrammetry and Remote Sensing*, 65(1), 2-16.

Blaschke, T., Burnett, C., Pekkarinen, A. (2004). New contextual approaches using image segmentation for object-based classification. In: De Meer, F., de Jong, S (Eds.), *Remote Sensing Image Analysis: Including the spatial domain* (pp. 211–236)., Kluver Academic publishers, Dordrecht.

Blaschke, T., Lang, S., Hay, G.J. (2008). *Object- Based Image Analysis- Spatial concepts for knowledge driven remote sensing applications*. Springer, Heidelberg, Berlin, New York.

Clinton, N., Holt, A., Scarborough, J., Yan, L., Gong, P. (2010). Accuracy assessment measure for object-based image segmentation goodness. *Photogrammetric Engineering and Remote Sensing*, 76, 289–299.

Çölkesen, I., Kavzoğlu, T. (2017) The use of logistic model tree (LMT) for pixel- and object-based classifications using high-resolution WorldView-2 imagery. *Geocarto International*, 32, 71-86.

Esetlili, M, Bektas Balcik, F., Balik Sanli, F., Kalkan, K., Ustuner, M., Goksel, C., Gazioğlu, C., Kurucu, Y. (2018). Comparison of Object and Pixel-Based Classifications For Mapping Crops Using Rapideye Imagery: A Case Study Of Menemen Plain, Turkey. *International Journal of Environment and Geoinformatics,* 5(2), 231-243. DOI: 10.30897/ijegeo.442002

Espindola, G.M., Camara, G., Reis, I.A., Bins, L.S., Monteiro, A.M. (2006). Parameter selection for region-growing image segmentation algorithms using spatial autocorrelation. *International Journal of Remote Sensing*, 27(14), 3035–3040.

Gao, Y., Mas, J. F., Kerle, N., Navarrete Pacheco, J. A. (2011). Optimal region growing segmentation and its effect on classification accuracy. *International Journal of Remote Sensing*, 32(13), 3747-3763.

Grybas, H., Melendy, L., Congalton, R.G. (2017). A comparison of unsupervised segmentation parameter optimization approaches using moderate-and high-resolution imagery. *GIScience Remote Sensing*, 54(4), 515-533.

Hossain, M.D., Chen, D. (2019). Segmentation for object-based image analysis (OBIA): A review of algorithms and challenges from remote sensing perspective. *ISPRS Journal of Photogrammetry and Remote Sensing*, 150, 115-134.

Jensen, J.R. (2016). *Introductory digital image processing: a remote sensing perspective*. 4th ed. Upper Saddle River, NJ: Pearson Prentice Hall.

Johnson, B., Bragais, M., Endo, I., Magcale-Macandog, D., Macandog, P. (2015). Image segmentation parameter optimization considering within- and between-segment heterogeneity at multiple scale levels: test case for mapping residential areas using Landsat imagery. *ISPRS International Journal of Geo-Information*, 4, 2292-2305.

Johnson, B., Xie, Z. (2011). Unsupervised image segmentation evaluation and refinement using a multi- scale approach. *ISPRS Journal of Photogrammetry and Remote Sensing*, 66(4), 473-483.

Kavzoğlu, T. (2017). Object-Oriented Random Forest for High Resolution Land Cover Mapping Using Quickbird-2 Imagery. In: Samui, P., Sekhar, S., Balas, V. E. (Eds.), *Handbook of Neural Computation* (pp. 607-619), Elsevier.

Kavzoğlu, T., Çölkesen, I. (2013). An assessment of the effectiveness of a Rotation Forest ensemble for land-use and land-cover mapping. *International Journal of Remote Sensing*, 34(12), 4224-4241.

Kavzoğlu, T., Tonbul H. (2018). An Experimental Comparison of Multi-Resolution Segmentation, SLIC and K-Means Clustering for Object-Based Classification of VHR Imagery. *International Journal of Remote Sensing*, 39(18), 6020-6036.

Kavzoğlu, T., Yildiz Erdemir, M. and Tonbul, H. (2017). Classification of semiurban landscapes from very high-resolution satellite images using a regionalized multiscale segmentation approach. *Journal of Applied Remote Sensing*, 11(3), 035016.

Martha, T.R., Kerle, N., van Westen, C.J., Jetten, V., Kumar, K.V. (2011). Segment optimization and data-driven thresholding for knowledge-based landslide detection by object-based image analysis. *IEEE Transactions on Geoscience and Remote Sensing*, 49, 4928-4943.

Saba, F., Zoej, M.J.V., Mokhtarzade, M. (2016). Optimization of Multiresolution Segmentation for Object-Oriented Road Detection from High-Resolution Images. *Canadian Journal of Remote Sensing*, 42, 75-84.

Su, T. (2019). Scale-variable region-merging for high resolution remote sensing image segmentation. *ISPRS Journal of Photogrammetry and Remote Sensing*, 147, 319-334.

Tonbul, H., Kavzoğlu, T. (2019). Application of Taguchi Optimization and ANOVA Statistics in Optimal Parameter Setting of MultiResolution Segmentation. *Proc. Symposium on 9th Recent Advances in Space Technologies (RAST)*, Istanbul, Turkey, 387-391.

Yang, J., He, Y., Weng, Q. (2015). An automated method to parameterize segmentation scale by enhancing intrasegment homogeneity and intersegment heterogeneity. *IEEE Geoscience Remote Sensing Letters*, 12 (6), 1282-1286.

Zhang, H., Fritts, J., Goldman, S. (2008). Image segmentation evaluation: a survey of unsupervised methods. *Computer Vision and Image Understanding*, 110(2), 260-280.

Zhang, Y.J., 1996, A survey on evaluation methods for image segmentation. *Pattern Recognition*, 29(8), 1335-1346..